Anatomy of the murine and human cochlea visualized at the cellular level by synchrotron-radiation-based microcomputed tomography

B. Müller*[a], A. Lareida*[a], F. Beckmann[b], G. M. Diakov[c], F. Kral[c], F. Schwarm[c], R. Stoffner[d], A. R. Gunkel[e], R. Glueckert[e], A. Schrott-Fischer[e], J. Fischer[f], A. Andronache[a], and W. Freysinger[c]
[a]Computer Vision Lab, ETH Zurich, Sternwartstrasse 7, 8092 Zürich, SWITZERLAND; [b]GKSS-Research Center, 21502 Geesthacht, GERMANY; [c]4D Visualization Laboratory, Innsbruck Medical University, Anichstrasse 35, 6020 Innsbruck, AUSTRIA; [d]University Clinic of Radiology I, Innsbruck Medical University, Anichstr. 35, 6020 Innsbruck, AUSTRIA; [e]University Clinic of Oto-, Rhino-, Laryngology, Innsbruck Medical University, Anichstrasse 35, 6020 Innsbruck, AUSTRIA; [f]Clinic of Orthopaedic Surgery, Hannover Medical School, 30625 Hannover, GERMANY; *present address: University of Basel, Spitalstrasse 21, 4031 Basel, SWITZERLAND

ABSTRACT

Diseases of the hearing organ and impairment affect a significant fraction of population. Therefore, the hearing organ embedded as a helical structure in the cochlea within the hardest human osseous structure inside the petrous bone is intensively investigated. Currently, studies of the cochlea with true micrometer resolution or better are destructive. Membranes and three-dimensional vessel structures of post-mortem explanted human cochlea were only visualized with limited spatial resolution or deformed anatomical features resulting from preparation artifacts. We have applied a preparation and staining protocol developed for electron microscopy, which allows the visualization and quantification of a great variety of soft-tissue structures including the Reissner´s membrane, the tectorial membrane, basilar membrane, modiolus, lamina radialis, and Nuel´s space by the use of synchrotron-radiation-based micro computed tomography at the beamline BW 2 (HASYLAB at DESY). The level of detail can be even improved by the application of sophisticated computer vision tools, which enables the extraction of the vascular tree down to the capillaries and of the course of nerve fibers as well as the topology of the osseous lamina radialis, which assembles the nerve fibers from the hair-cells to the ganglia in the center of the cochlea, the modiolus. These non-destructively obtained three-dimensional data are principal for the refined understanding of the hearing process by membranes morphologies and further anatomical features at the cellular level and for teaching purposes in medical curricula.

Keywords: Human cochlea, synchrotron radiation, micro-computed tomography, differential absorption contrast, segmentation, histology, 3D-Slicer

1. INTRODUCTION

The human hearing apparatus has found attention for a wide community. Due to the anatomical, biochemical and functional complexity of human hearing organ with microscopic and densely packed structures and its relevance for human's daily life it is subject to intensive research.[1]

Conventional computed tomography (CT) is widely used as powerful medical imaging tool in diagnostics. Specifically well, bone surrounded by different kind of soft tissues can be visualized down to the sub-millimeter level. The standard CT in absorption contrast mode, however, has intrinsically low soft tissue differentiation power. Therefore, other modalities such as magnetic resonance tomographic imaging (MRI) have to be used in addition. Unfortunately these modalities provide very limited spatial resolution and thus cannot be used for imaging of cellular features with weak absorption contrast, as is the human hearing organ - the Organ of Corti with its micrometer-thin membranes, capillaries, individual cells and substructures.

*bert.mueller@unibas.ch; phone +41 61 265 9660

Developments in X-Ray Tomography V, edited by Ulrich Bonse,
Proc. of SPIE Vol. 6318, 631805, (2006) · 1605-7422/06/$15 · doi: 10.1117/12.680540

Many aspects of the organ of Corti have been studied and more or less well understood. The structure of the vascular tree in the cochlea nourishing the organ of Corti, however, is still hardly known. Imaging the vascular structures of an organ is often based on the injection of contrast agents. Depending on the application protocol, arterial or venous phases are documented in the living human. Partly, this is due to the fact that extreme high-resolution imaging is impossible with living persons. Post mortem, the smaller vessels and especially the capillaries under consideration almost immediately clot with blood and cannot be filled with the known contrast agents any more. Furthermore, the cochlea, hosting the organ of Corti, is located in the hardest human bone, the petrous bone, in the center of the head, which makes the studies extremely difficult.

High-resolution CT investigations cannot be performed in vivo, since the high doses create non-tolerable damages. The high-resolution studies of the anatomy are, therefore, ex vivo, post mortem investigations based on histological sections and different staining protocols. For these immuno-histochemical, (electron-)microscopic studies the cochlea has to be destroyed. This is often related to the loss of spatial resolution in the third direction. Alternatively, it has been proposed to use the synchrotron-radiation-based micro computed tomography (SRμCT), which is non-destructive and provides a spatial resolution down to the sub-cellular level. This technique is appropriate for a detailed study of the cochlea and the organ of Corti itself with equidistant, homogeneous, true micrometer resolution in the three orthogonal directions.

The spatial resolution of SRμCT that corresponds to about 1 μm is ideally apt for investigating the vascular system in dedicated parts of the cochlea, namely in segments of the cochlea from the center of the spiral radially out, in the direction of the hair-cells, which mechano-electrically convert sound into neural pulses. The organ of Corti, a highly complex arrangement of inner and outer hair cells, is responsible for this signal transformation. The electric signals are transported to the modiolus, the center of the cochlea, from where they are collected, transported and processed on the way to the hearing cortex. This whole process is extremely dependent on a continuous supply with nutrients including oxygen and sugar. The disturbances of the cochlear arterial microcirculation are suspected to cause tinnitus, hearing deficits, and deafness. Thus it is clear that the structure of the microscopic vascularization of the hearing organ is of crucial relevance.

2. MATERIALS AND METHODS

2.1 Preparation of the cochlea for SRμCT measurements

Preliminary SRμCT-experiments have shown that freshly explanted cochleae from untreated human cadavers do not exhibit a sufficiently high x-ray absorption contrast to visualize the tiny features of the soft-tissue structures of the organ of Corti.[2] Therefore, suitable staining protocols have to be applied.

The cochleae were explanted from human and rodent cadavers in a suitable time window post mortem, prior to the onset of lytic destructive processes. The bony hull was drilled away as much as possible but without destroying the cochlea itself. The specimens were fixated in Karnovsky's formaldehyde-glutaraldehyde solution. Subsequently, the specimens were postfixated with 1% OsO_4 for 45 minutes and finally embedded in SPURR's low viscosity epoxy resin.[3,4]

2.2 Synchrotron-radiation-based micro computed tomography (SRμCT)

The SRμCT-measurements were performed using the standard set-up for absorption contrast at the beamlines BW 2 and W 2 (HASYLAB at DESY, Hamburg, Germany), synchrotron radiation sources of the second generation.[5] Since the monochromatic synchrotron radiation was almost perfectly parallel, the tomograms were reconstructed slice-wise based on the filtered back-projection algorithm.[6] For the characterization of the specimens at the beamlines different photon energies were applied as indicated in the figure captions. 720 projections between 0 and 180° were recorded with moderate optical magnifications. The spatial resolution of the entire set-up was experimentally characterized measuring the modulation transfer function. Here, we used the projection of the sharp edge of a gold plate recorded under the conditions applied for the data acquisition.[7]

2.3 Image processing of the SRμCT data

The SRμCT data from the beamline BW 2 lead to histograms of the local absorption coefficients that have exactly the Gaussian shape.[8] Therefore, it is relatively simple to determine the threshold for the purely intensity-based segmentation of the different components of interest. The software VG Studio Max (Volume Graphics, Heidelberg, Germany) served for the 3D visualization of the blood vessel system in the cochlea.

For the segmentation and visualization of the membranes we used the open-source ITK and VTK based 3D-Slicer[9] that was ported to a 64-bit Linux operating system (Yellow Dog Linux 4.1, on a dual processor machine with 8 GB RAM, Apple G5 dual, 2.7 GHz, Radeon 9650, 256 MB RAM graphics card). This configuration can handle image stacks under consideration, approximately 1k slices with 2.3 MB each (TIFF). 3D-segmentation, interaction and visualization became reasonable with this environment. The segmentations were done under Mac OSX 10.4 (OS X) & Yellow Dog Linux 4.1 (YDL). The compilations were done with gcc 3.3, native Carbon.GUI – 3D graphics acceleration for OS X, gcc 4.1, native X-windows – no 3D-graphics acceleration for YDL; VTK 5.0 / ITK 2.6 were used as open-source image processing libraries; CMake, compilation as shared libraries with hybrid, patented, Tcl-wrapping and the same compiler options for all libraries. These resources can be tracked from http://www.slicer.org.

2.4 Differential absorption contrast measurements

In order to extract the morphology of the components of interest, only the single energy monochromatic beam is generally used. The photon energy is adapted to the sample diameter and average composition, which provides the total x-ray absorption. The aim is to minimize the time for the data acquisition given by a semitransparent specimen.[10]

One of the main advantages of SRμCT with respect to classical μCT in the laboratory is the tunable source that gives rise to the reasonable photon flux of energies within a window of 10^{-4}. Therefore, one can take advantage measuring two tomograms above and below the desired absorption edge of the specific element such as osmium. The subtraction of the two 3D datasets results in the distribution of the osmium in the specimen. This only works well if any relative motion is avoided or the two datasets are appropriately registered.

The L3-edge subtraction of the Os-stained specimens utilizes the discontinuity in the absorption coefficient shown in Fig. 1. The absorption of osmium increases by more than the factor of 2 between 10.8 and 10.9 keV, while the absorption of the other components in the specimens stays almost constant. In order to obtain more precise results, one can easily incorporate rough estimates for the change of the total absorption between the two photon energies. Because the sensitivity for osmium is orders of magnitude higher than that for soft and hard tissues, images with only moderate osmium concentration can be acquired.

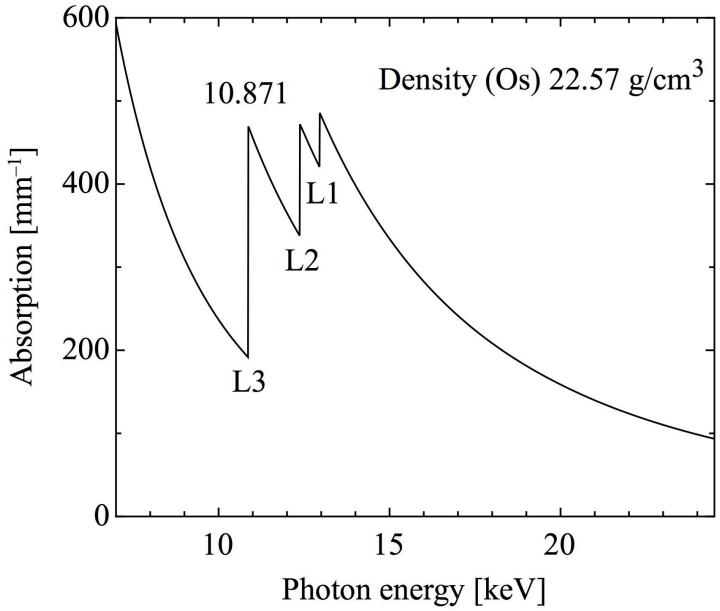

Fig. 1. The X-ray absorption of osmium with a density of 22.57 g/cm^3 versus photon energy. The absorption increases by more than a factor of 2 at the L3 line, which corresponds to the energy of 10.871 keV.

3. RESULTS

3.1 Registration of tomograms for differential contrast imaging

The spatial misalignment and misorientation between the two tomographic datasets was compensated using the conventional voxel-based rigid registration algorithm, i.e. the maximization of Mutual Information (MI) approach, as presented in Refs. 11 and 12. The necessary transformation was defined with six degrees of freedom - three translations and three rotations, as the specimen is solid. However, even though both 3D datasets are obtained within the same setup, the change of the photon energy and the sample manipulation by many rotation and translation movements between the comparable acquisitions causes the multi-modal characteristics to the registration process. Therefore, MI is needed to define the similarity measure between the images and to quantify the goodness of match. The MI is estimated from the joint intensity histogram using 256 bins and tri-linear voxel interpolation, as presented.[12] The six registration parameters, corresponding to the aforementioned degrees of freedom and defining the rigid registration transformation, are optimized using the Powell multi-dimensional search algorithm[13] such that the MI between the two images is maximized.

The registration using a reference image of 512 x 512 x 575 voxels and a floating image of 512 x 512 x 423 voxels validates that the rotation axes fit perfectly, whereby the transformation for the 3 translation parameters is of sub-voxel size. The registration process took approximately 4 hours on a SunBlade 1500.

Fig. 2 shows typical slices of the murine cochlea parallel to the rotation axis. This embedded cochlea is significantly smaller than human ones and, therefore, has the appropriate diameter to be visualized in absorption contrast mode using photon energies of about 11 keV. The murine cochlea is much easier available than the human ones and is often applied as the suitable model system. The slice on the left exhibits higher absorption than the one in the center, which was received just below the absorption edge L3 of osmium, which indicates a relevant Os content. The spatial distribution of osmium is represented on the right. The concentrations are well below 1‰. The gray values clearly verify that the sensitivity for osmium in the hard and soft tissue of the cochlea is several 10^{-5}.

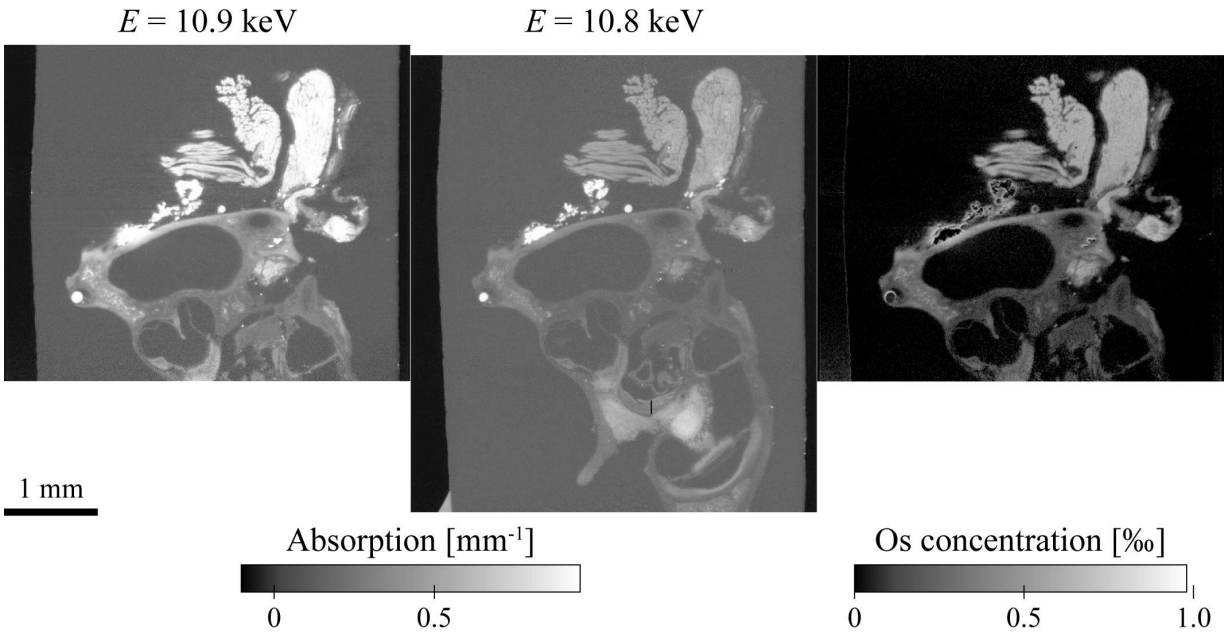

Fig. 2. Slices obtained from the Os-stained murine cochlea. On the left, the slice parallel to the rotation axis produced out of two tomograms measured with the photon energy of 10.9 keV shows many features with high contrast. The slice in the center exhibits much less absorption, although it is obtained using just a 100 eV lower photon energy. On the right, the slice is the difference image after registration, which represents the local osmium distribution in the specimen.

3.2 Anatomy of the murine cochlea

The cochlea with its coiled shape serves for the transition of mechanical (sound) to electrical signals, which takes place in the core component, the organ of Corti, see lower part in Fig. 3. The modiolus, which is the central bony pillar of the cochlea, is represented on the right 3D image, which is generated by subsequent cutting in 0.5 mm steps. The image width and height correspond to 3.4 mm and 4.8 mm, respectively. The depth of the images changes from 3.2 mm, 2.8 mm, via 2.3 mm to 1.8 mm. The detailed analysis of the anatomic features is ongoing and will be published in a forthcoming paper.[14]

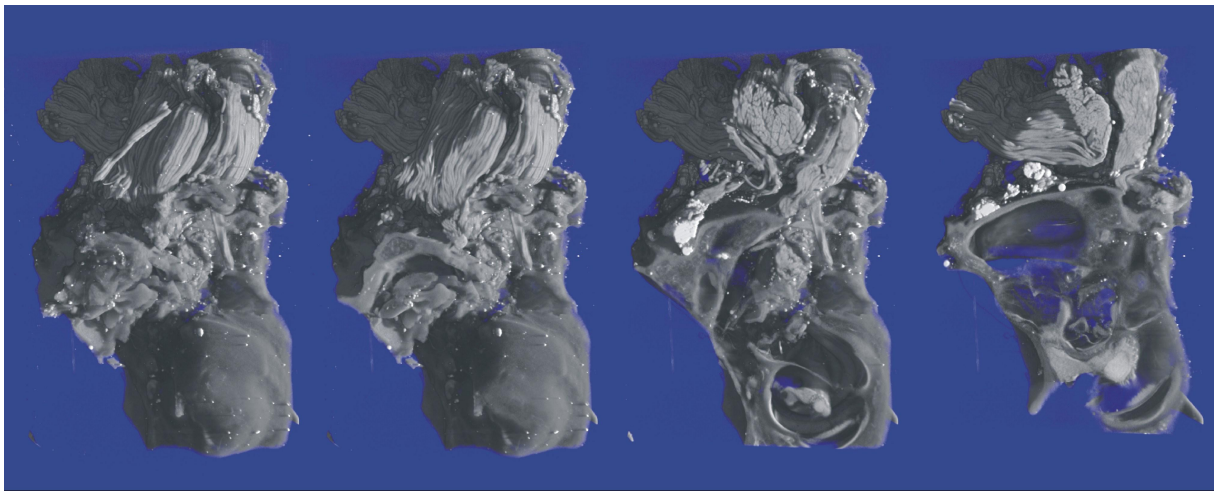

Fig. 3. The 3D images show the murine cochlea. As the result of the osmium tetroxide fixation, not only the bony tissue but also the soft tissues exhibit bright contrast. Many details can be extracted as seen by the subsequent cuts in depth. The measurement was performed using the photon energy of 10.8 keV. The voxel size corresponds to 2.8 µm and the spatial resolution to 5.2 µm.

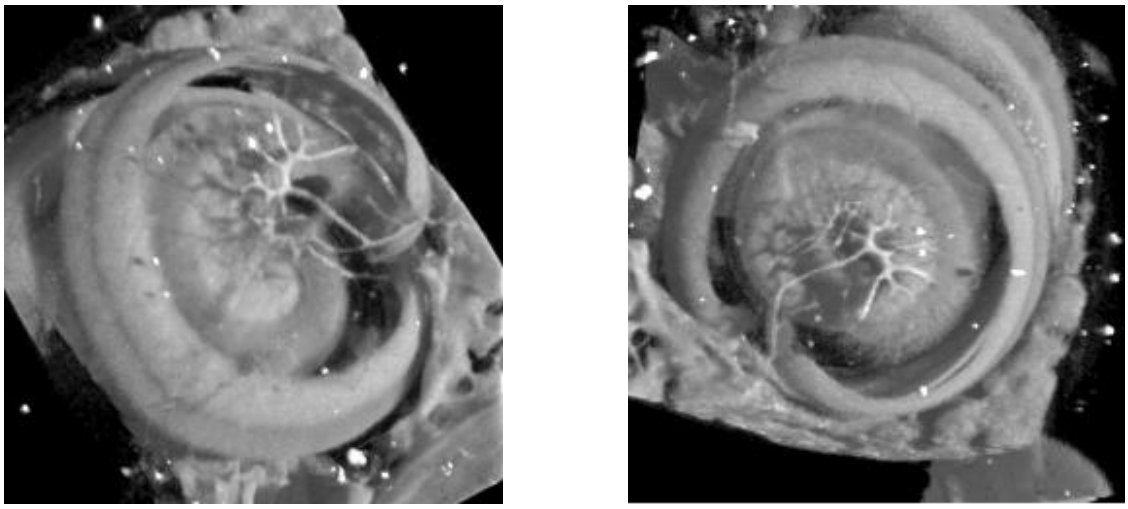

Fig. 4. The 3D representation of blood vessels supplying the apical vascular network of the murine cochlea. The parameters for the measurement correspond to the ones given in the caption of Fig. 3.

The vascular nutrition is secured by the inferior posterior cerebellar artery, which originates from the basilar artery and crosses the inner ear channel together with the eighth cranial nerve. In the inner ear, the cerebellar artery bifurcates into

several branches. On the images in Fig. 4, one can see the branch supplying the apical vascular network of the cochlea. Below the vessel tree one can recognize the apical winding of the cochlea. This 3D representation with a spatial resolution of about 5 μm is based on measurements using the photon energy of 10.8 keV. The voxel length corresponds to 2.82 μm. This spatial resolution allows the visualization of the smallest blood vessels, which are the capillaries.

3.3 Membranes of the human cochlea

The images in Figs. 5 and 6 demonstrate that we have non-destructively obtained tomograms that reveal the complex anatomy of the human hearing organ with the spatial and density resolution almost comparable to histological sectioning. There is no other non-invasive technique available with a spatial resolution comparable to histological sections. Since the morphology of the membranes can drastically change as the result of the cutting. The embedding of the cochlea may reduce the shape changes, but the influence of preparation artifacts is still unknown. In the following, we concentrate on the different membranes in the cochlea, which are often just one or two cell layers thick.

The slice in Fig. 5 shows Reissner's membrane (vestibular membrane), which separates the scala vestibuli and the cochlear duct. This membrane is composed of two cell layers, one epithelial and one mesothelial cell layer, supported by a basal lamina. Together with the basilar membrane it forms the compartment inside the cochlea, the cochlear duct, which is filled by endolymph, an extracellular fluid important for the function of the organ of Corti.

The tectorial membrane consists of an anisotropic composite of thin fibers in a semisolid matrix. It is composed of collagens and other molecules, forming the fibers and the matrix. This membrane acts as the vibrating mechanism in the cochlea and is incredibly delicate and flexible. The anisotropy results in much higher flexibility in transverse than in longitudinal direction. The skinny inner part of the tectorial membrane overlies interdental cells at the spiral limbus and terminates into the marginal net with delicate protrusions.[15] The shape of the tectorial membrane is nicely seen in the tomogram. The anisotropy, which is based on nanometer scale features, however, is invisible.

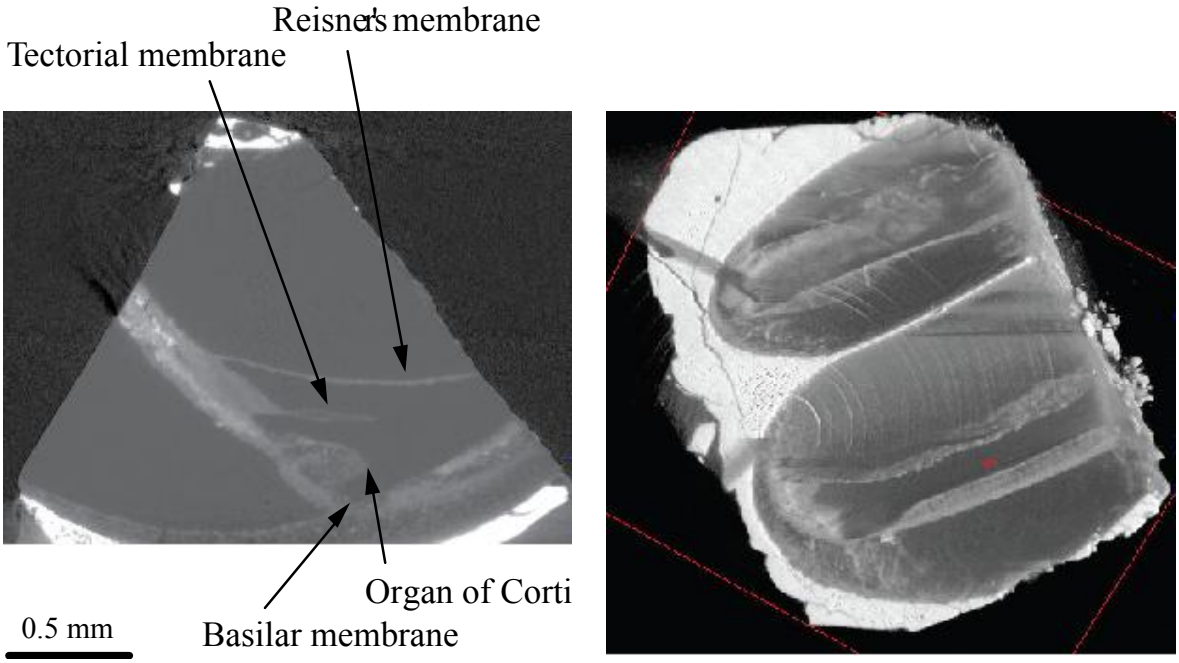

Fig. 5. The slice on the left demonstrates the power of SRμCT uncovering cellular anatomic features inside the cochlea including the Reissner,s membrane, the tectorial membrane, the basilar membrane as well as the organ of Corti. The 3D representation on the right shows the membranes in the middle and apical turn on coarser scale. Inside the two turns one sees the cochlear duct, which is filled with endolymph and defined by the Reissner's membrane on the upper side and the basilar membrane on the lower one.

The organ of Corti (spiral organ) is a rather complex structure that responds to vibrational fluid movements in the cochlea. It contains the hair cells that act as the auditory sensors. Shear on these hair cells can open ion channels. This

process is associated with neural, electrical signals transmitted to the auditory cortex. The organ of Corti contains also other cells, which are present in the tomographic data. The detailed analysis is not finalized yet and will be the focus of a forthcoming paper. [16]

The basilar membrane provides the fundament for the organ of Corti. It separates the scala media and scala tympani, cavities, which run along the coil of the cochlea. Therefore, the basilar membrane organizes the hair cells in a fashion that they are adjacent to endolymph and perilymph, a condition for their function. Endolymph and perilymph are liquids with a different potassium concentration, which results in a difference of the electrical potential. This allows the flow of ions, mainly potassium, after activation. Leakage can cause disruption or breakdown of hearing.

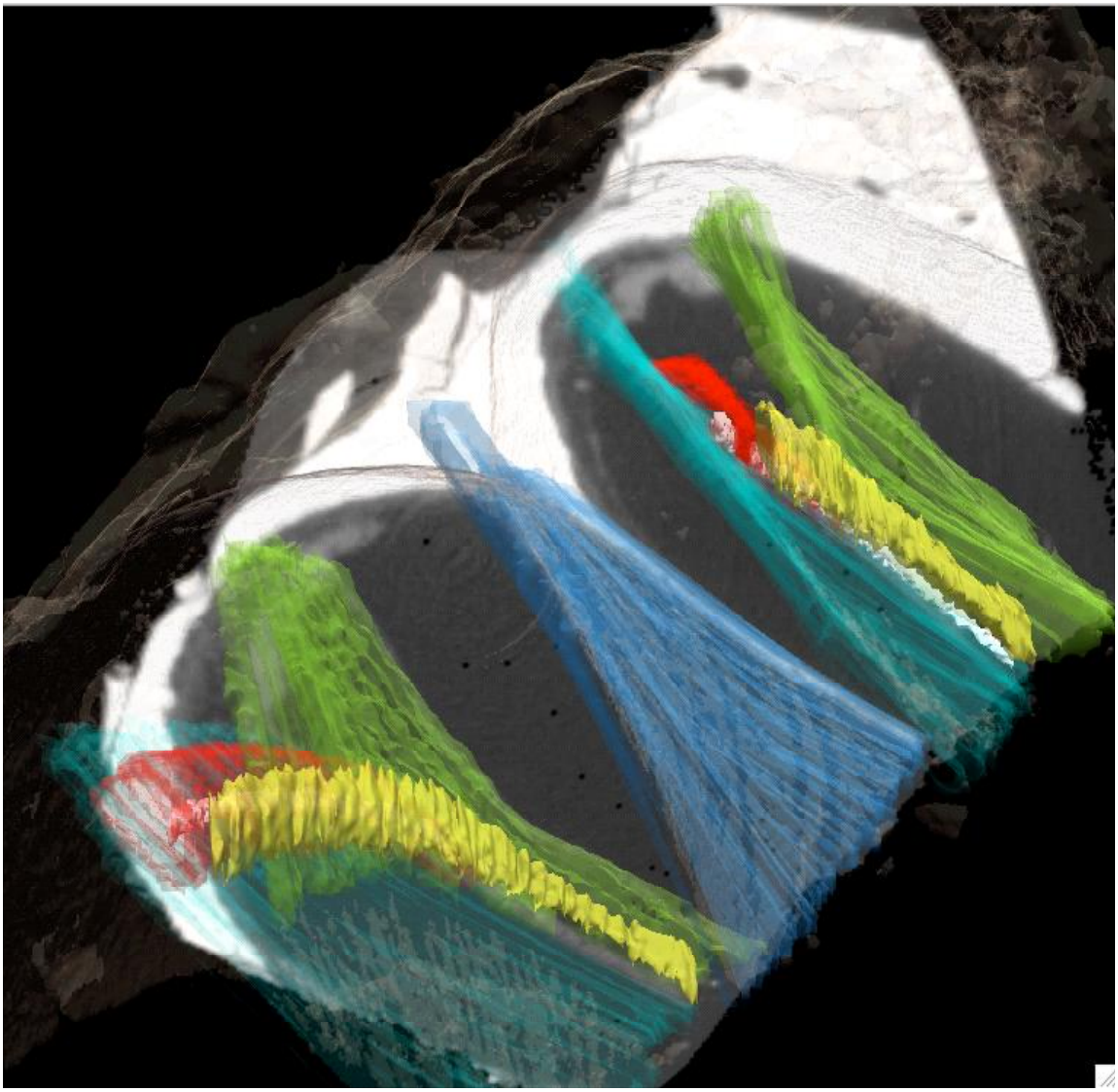

Fig. 6. The 3D-Slicer enables us to segment the anatomical features including the membranes and describe them using the color code. The Reissner's membrane is green-colored. The organ of Corti and the Nuel's space are shown in red and white, respectively. The tectorial and the basilar membranes are given in yellow and turquoise. The thin bony interface between the windings is blue-colored.

Fig. 6 shows the segmented anatomical features including the membranes in different colors. The Reissner's membrane and organ of Corti are green- and red-colored, respectively. The tectorial and the basilar membranes are given in yellow

and turquoise. The Nuel's space is shown in white. It is the name of the interval between the outer pillar cells, the outer phalangeal cells and outer hair cells. The thin bony tissue between the windings is blue-colored. The outer bone is hold in white and provides the 3D basis for the attachment of the different membranes.

4. DISCUSSION

SRμCT in absorption contrast mode allows the imaging of the cochlea and the adjacent tissues with isotropic spatial resolution down to the cellular level. Single- and double cell-layer membranes can be extracted if an appropriate specimen preparation protocol including staining with species like osmium is applied. It is possible to investigate the morphology of the different membranes in 3D space interactively. Even without elaborate data treatment, smoothing and filtering the 3D shape of the membranes becomes to light. Consequently, SRμCT gives rise to results comparable to classical histology. It should be noted, however, that SRμCT is not expected to replace histology but provide complementary information, as histology also allows direct relationship to the cell performance and function.

Specimens with suitable diameter allow analyzing the spatial distribution of a selected element taking advantage of the differential absorption contrast. The sensitivity for osmium within the stained cochlea, e.g., corresponds to several 10^{-5}. The tuning of the photon energy is a major advantage of SR sources with respect to the laboratory bremsstrahlung sources.

The presented data of the cochlea allow obtaining volumetric and morphological data at high resolution, important for the ultra-structural evaluation using sections. This is especially essential for membranes and micro-vascular structure. The precise data are also the basis for sophisticated flow simulations. Once a reasonable number of pathologic and healthy cases are acquired, the desired therapeutic paths to treat sudden and age-related hearing loss, tinnitus, etc. can be selected. The data will be also used for the fabrication of 3D models of the murine and the human specimens for teaching purposes on a more detailed level than today.[17]

ACKNOWLEDGMENT

The work was performed within the framework of approved proposals of HASYLAB at DESY. The support of the European Community - Research Infrastructure Action under the FP6 "Structuring the European Research Area" Programme through the Integrated Infrastructure Initiative "Integrating Activity on Synchrotron and Free Electron Laser Science", Austrian Science Foundation FWF project P15948-B05, and Austrian National Bank, The Jubilee Fund, under Project 9318 is gratefully acknowledged.

REFERENCES

1. R. Yehoash and R.A. Altschuler, "Structure and innervation of the cochlea", Brain Research Bulletin **60**, 397–422 (2003).
2. U. Vogel, "New Approach for 3D imaging and geometry modelling of the human inner ear", ORL **61**, 259-267 (1999).
3. H. Spoendlin and A. Schrott, "The spiral ganglion and the innervation of the human organ of Corti", Acta Otolaryngol. **105**(5-6), 403-410 (1988).
4. H. Spoendlin and A. Schrott, "Analysis of the human auditory nerve", Hear Res. **43**(1), 25-38 (1989).
5. F. Beckmann, in *Developments of X-ray tomography III*, edited by U. Bonse (SPIE- The International Society for Optical Engineering, San Diego, USA), Vol. **4503**, 34-42 (2001).
6. A.C. Kak and M. Slaney, *Principles of computerized tomographic imaging*, Society of Industrial and Applied Mathematics, 2001.
7. B. Müller, P. Thurner, F. Beckmann, T. Weitkamp, C. Rau, R. Bernhardt, E. Karamuk, L. Eckert, S. Buchloh, E. Wintermantel, D. Scharnweber, H. Worch, in *Developments of X-ray tomography III*, edited by U. Bonse (SPIE-The International Society for Optical Engineering, San Diego, USA), Vol. **4503**, 178-188 (2001).
8. B. Müller, F. Beckmann, M. Huser, F. Maspero, G. Szekely, K. Ruffieux, P. Thurner, E. Wintermantel, "Non-destructive three-dimensional evaluation of a polymer sponge by micro-tomography using synchrotron radiation" Biomol. Eng. **19**, 73-78 (2002).

9. A. Nabavi, P.M. Black, D.T. Gering, C.F. Westin, V. Mehta, R.S. Pergolizzi Jr, M. Ferrant , S.K. Warfield , N. Hata, R.B. Schwartz, W.M. Wells 3rd, R. Kikinis, F.A. Jolesz, "Serial intraoperative magnetic resonance imaging of brain shift", Neurosurgery **48**(4), 787-797, discussion 797-798, (2001).
10. L. Grodzins, "Optimum Energies for X-ray Transmission Tomography of Small Samples - Applications of Synchrotron Radiation to Computerized Tomography I", Nucl. Instrum. Meth. **206**, 541-545 (1983).
11. P. Viola and W.M. Wells III, "Alignment by maximization of mutual information", ICCV '95: Proceedings of the Fifth International Conference on Computer Vision (IEEE Computer Society), 16 (1995).
12. F. Maes and A. Collignon , D. Vandermeulen, G. Marchal and P. Suetens, "Multi-modality image registration by maximization of mutual information", Proc. IEEE Workshop Mathematical Methods in Biomedical Image Analysis, 14-22 (1996).
13. H.W. Press, B.P. Flannery, S.A. Teukolsky, and W.T. Vetterling, *Numerical Recipes in C - The Art of Scientific Computing*, Cambridge University Press 1988.
14. A. Lareida et al., in preparation.
15. R. Glueckert, K. Pfaller, A. Kinnefors, A. Schrott-Fischer, and H. Rask-Andersen., "High resolution scanning electron microscopy of the human organ of Corti.: A study using freshly fixed surgical specimens", Hearing Research **199**, 40–56 (2005).
16. W. Freysinger et al., in preparation.
17. W. Haobing, C. Northrop, B. Burgess, M.C. Libermann, S.N. Merchant, "Three-dimensional virtual model of the human temporal bone: a stand-alone, downloadable teaching tool", Otol. Neurotol. **27**, 452 – 457 (2006).